ELSEVIER

Journal of Organometallic Chemistry 659 (2002) 1–9

Journal of Organometallic Chemistry

www.elsevier.com/locate/jorganchem

Cationic ruthenium(II) complexes containing a chelating η^1:η^6-phosphinoarene ligand; [RuCl(L)($PPh_2(CH_2)_3$-η^6-C_6H_5)][PF_6] (L = $P(OPh)_3$, $P(OMe)_3$, PPh_3, PMe_3, NCMe, NC_5H_5)

Paul D. Smith [a,*], Thomas Gelbrich [b], Michael B. Hursthouse [b]

[a] Department of Chemistry and Materials, Manchester Metropolitan University, Manchester M1 5GD, UK
[b] Department of Chemistry, EPSRC National Crystallography Service, University of Southampton, Highfield, Southampton SO17 1BJ, UK

Received 16 April 2002; received in revised form 16 May 2002; accepted 16 May 2002

Abstract

Reactions of the ruthenium(II) complex [$RuCl_2(PPh_2(CH_2)_3$-η^6-C_6H_5)], containing a chelating η^1:η^6-phosphinoarene ligand, with NH_4PF_6, in the presence of a variety of neutral two-electron donor ligands, have yielded a series of new cationic complexes of the general formula [RuCl(L)($PPh_2(CH_2)_3$-η^6-C_6H_5)][PF_6] [L = $P(OPh)_3$ (**1**), $P(OMe)_3$ (**2**), PPh_3 (**3**), PMe_3 (**4**), NCMe (**5**), NC_5H_5 (**6**)]. The structures of complexes **3** and **5** have been determined by X-ray crystallography. In all cases ^{1}H- and $^{13}C\{^1H\}$-NMR spectra showed characteristic upfield chemical shifts indicative of the presence of a π-bound arene ligand. The η^6-C_6H_5 group displayed five inequivalent resonances in the ^{1}H-NMR spectra, in most cases showing three triplets and two doublets (vicinal coupling, $^3J_{HH}$ = 6.4–5.4 Hz) of relative intensities 1:1:1:1:1 and six peaks were observed for the η^6-C_6H_5 ligand in the respective $^{13}C\{^1H\}$-NMR spectra, consistent with C_1 molecular symmetry at the ruthenium centre in solution. Detailed assignment of the η^6-arene resonances has been achieved using a collection of ^{1}H–^{1}H COSY and ^{1}H–^{13}C correlation experiments, combined with a consideration of the relative magnetic anisotropic shielding and the *trans* influence effects attributed to the ligands L.

Keywords: Arene; Chelating ligand; Phosphine; Ruthenium

1. Introduction

The varied array of arene–ruthenium complexes known is largely due to the strong arene–metal bond, in addition to the availability of reactive arene-containing compounds and the ready accessibility of both Ru(II) and Ru(0) oxidation states [1]. Arene–ruthenium complexes are important precursors for catalytic hydrogenation reactions [2] and have established an increasingly significant role in organic synthesis and homogeneous catalysis [3]. One of the critical reactions in catalytic cycles can involve the progressive removal of the arene group from η^6 to η^4 and η^2, however, the complete disengagement of the arene may be an unwanted side reaction. An obvious way of preventing ring loss during reactions is to tether the arene moiety on to another pendant donor atom and hence capitalise on the chelate effect. Mirkin et al. have previously reported tethered η^6-arene–Rh(I) complexes using the eight-electron donor ligand $Ph_2PCH_2CH_2OPh$ [4] and in recent years there have been a number of chelated η^6-arene–Ru(II) complexes published in the literature [5–18]. These complexes have provided a challenge in both the synthesis of new ligands and new methods for preparing organometallics. Examples of tethered η^6-arene–Ru(II) complexes have now been prepared which contain a η^6-arene ring strapped to a variety of pendant donor atoms such as, carbene [5], pyrazole [6], alcohol [7], phosphine [8–15] thioether [16], arsine [17] and pyrazole–phosphine groups [18]. Thermogravimetric analysis and ^{1}H-NMR spectroscopy have demonstrated that Ru(II) complexes containing a chelating arene–phosphine ligand are significantly more stable towards arene displacement than their non-chelating counterparts [10b]. This study has examined the effects of a

* Corresponding author. Fax: +44-161-2476357
E-mail address: p.smith@mmu.ac.uk (P.D. Smith).

0022-328X/02/$ - see front matter
PII: S0022-328X(02)01591-7

chelating phosphinoarene moiety since they provide a rigid ligand framework by bonding to the metal in a (η^1:η^6) fashion [8–15]. The synthesis of [$RuCl_2(PPh_2(CH_2)_3$-η^6-$C_6H_5)$], via a thermal arene-substitution reaction, provided a convenient route to a new chelated arene–phosphine–Ru(II) complex [8]. Further work has now explored the reactions of this complex with NH_4PF_6, in the presence of a variety of neutral two-electron donor ligands using similar procedures to those previously described in the literature [19]. These reactions have afforded a range of new chiral 18 electron Ru(II) '*half-sandwich*' style cationic derivatives, [$RuCl(L)(PPh_2(CH_2)_3$-η^6-$C_6H_5)$][PF_6] [L = $P(OPh)_3$ (**1**), $P(OMe)_3$ (**2**), PPh_3 (**3**), PMe_3 (**4**), NCMe (**5**), NC_5H_5 (**6**)], which contain a chelated η^1:η^6-phosphinoarene ligand scaffold. A common characteristic of η^6-arene–ruthenium complexes of this type is various distortions to the co-ordinated arene ring, arising from electronic effects [20–22], which influence structural and spectroscopic properties. In all instances substantial upfield chemical shifts are observed in the ^{1}H- and $^{13}C\{^1H\}$-NMR spectra, which confirm the presence of a π-bound arene ligand [23,24]. This paper describes the synthesis, structures and NMR studies of complexes **1**–**6**. The NMR data has established the significance of these new chelating η^1:η^6-phosphinoarene–ruthenium complexes as excellent spectroscopic probes.

2. Results and discussion

2.1. Synthesis and characterisation

The mononuclear, cationic complexes **1**–**6** were isolated as yellow–orange, air-stable, high melting, non-hygroscopic, crystalline solids in good yield. All the compounds demonstrated good solubility in acetone and acetonitrile, but sparingly soluble in dichloromethane and chloroform, and insoluble in ether, hydrocarbons and alcohols. All ^{1}H-, $^{13}C\{^1H\}$- and $^{31}P\{^1H\}$-NMR spectra were recorded in d^6-acetone with the $[PF_6]^-$ counterion, in order to eliminate any potential solvent or anion effects. The proposed formulas were confirmed by microanalytical data. Complex **5** could be readily identified by the appearance of a ν(C≡N) stretching vibration at 2298 cm^{-1}.

2.2. Crystal structures

The molecular structures of complexes **3** and **5** have been determined by single crystal X-ray analysis and are shown with atom labelling in Figs. 1 and 2, respectively. Selected bond distances and angles are listed in Tables 1 and 2. The ruthenium centres in both complexes can be considered to possess pseudo-octahedral geometry, since the P(1)–Ru(1)–Cl(1), L–Ru(1)–Cl(1) and L–Ru(1)–P(1) angles are all ca. 90°, with the η^6-C_6H_5 ligand occupying three facial coordination sites. The Ru(1)–Cl(1) distances in **3** and **5** are comparable to similar complexes [25]. The Ru(1)–P(1) distances for **3** and **5** resemble those previously reported for related tethered η^1:η^6-phosphinoarene complexes [8,9,11,13,14,18a]. The

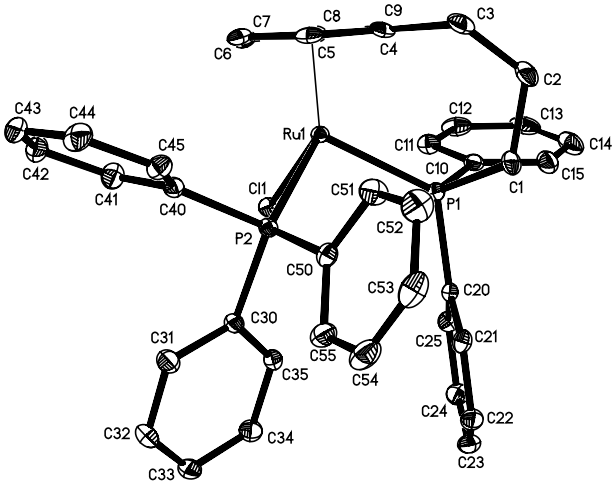

Fig. 1. ORTEP drawing of **3**. Hydrogen atoms have been omitted for chlarity.

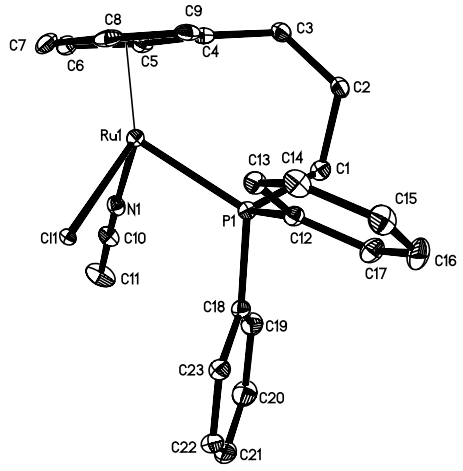

Fig. 2. ORTEP drawing of **5**. Hydrogen atoms have been omitted for chlarity.

Table 1
Selected bond lengths (Å) and angles (°) for **3**

Bond lengths			
Ru(1)–C(4)	2.243(3)	Ru(1)–C(9)	2.258(3)
Ru(1)–C(5)	2.225(3)	Ru(1)–Cl(1)	2.4000(8)
Ru(1)–C(6)	2.292(4)	Ru(1)–P(1)	2.3307(9)
Ru(1)–C(7)	2.282(4)	Ru(1)–P(2)	2.3718(9)
Ru(1)–C(8)	2.249(4)	$C–C_{(arene)}$	1.380(6)–1.431(5)
Bond angles			
P(1)–Ru(1)–P(2)	97.04(3)	P(2)–Ru(1)–Cl(1)	87.48(3)
P(1)–Ru(1)–Cl(1)	90.74(3)		

Table 2
Selected bond lengths (Å) and angles (°) for **5**

Bond lengths			
Ru(1)–C(4)	2.206(3)	Ru(1)–C(9)	2.196(3)
Ru(1)–C(5)	2.183(3)	Ru(1)–Cl(1)	2.4319(7)
Ru(1)–C(6)	2.249(3)	Ru(1)–P(1)	2.3218(9)
Ru(1)–C(7)	2.251(3)	Ru(1)–N(1)	2.046(3)
Ru(1)–C(8)	2.195(3)	C–$C_{(arene)}$	1.387(5)–1.428(5)
Bond angles			
P(1)–Ru(1)–N(1)	86.34(8)	N(1)–Ru(1)–Cl(1)	87.81(7)
P(1)–Ru(1)–Cl(1)	86.35(3)		

average Ru–$C_{(arene)}$ distances for **3** and **5** are 2.258(4) and 2.213(3) Å, respectively, which for **5** lie within the range expected for η^6-arene–Ru(II) complexes [20]. However, the average Ru(1)–$C_{(arene)}$ distances observed for **3** are notably longer than those anticipated for this class of organometallics. Although, the complexed aromatic rings in **3** and **5** are essentially planar there is significant buckling of the η^6-arene ligand where the Ru(1)–$C_{(arene)}$ distances *trans* to a P-donor are substantially greater than those *trans* to the Ru(1)–Cl(1) group. The asymmetric metal-ring bonding exhibited by these complexes has been attributed to the *trans* bond weakening properties of the tertiary phosphine [20]. The structural data obtained for **3**, Table 1, has shown that the η^1:η^6-phosphinoarene ligand exerts a greater *trans* influence than PPh_3, since the Ru(1)–C(6) and Ru(1)–C(7) distances are longer than the Ru(1)–C(8) and Ru(1)–C(9) distances, which lie *trans* to the PPh_3 ligand. This is consistent with the observed ruthenium–phosphorous bond lengths, where the Ru(1)–P(1) distance, labelled for the η^1:η^6-phosphinoarene moiety, is slightly shorter than the Ru(1)–P(2) bond assigned to the PPh_3 ligand. The steric constraints of the bulky PPh_3 group will hinder the approach of this ligand towards the metal, and account for the longer Ru(1)–P(2) distance relative to Ru(1)–P(1). A striking feature of the crystal structure for **3** was the longer Ru(1)–$C_{(arene)}$ distances compared to **5**, see Tables 1 and 2, in particular the Ru(1)–C(6) and Ru(1)–C(7) bonds, where the free end of the arene was significantly lifted from the ruthenium in **3**. This can be attributed to electronic factors and the steric influence of the PPh_3 ligand. In both **3** and **5**, the trigonal RuClPL fragment adopts a staggered arrangement relative to the carbon atoms of the aromatic ring. An examination of trimethylene straps in both complexes, showed co-planarity of the benzylic carbon atom, C(3), with the carbon atoms of the attached arene, without significant distortion of bond lengths or angles in the tether.

2.3. ^{1}H-NMR studies

The spectrum for $[RuCl_2(PPh_2(CH_2)_3$-η^6-$C_6H_5)]$ showed three well-separated peaks, one doublet at δ 5.16 ppm and two triplets at δ 5.77 and 6.39 ppm, of relative intensities 2:2:1 due respectively to the *ortho*, *meta* and para η^6-C_6H_5 ring protons [8]. This assignment may be interpreted on a first-order basis since H_{ortho} is strongly coupled only to H_{meta} and consistent with ideal C_s molecular symmetry at the metal centre in solution. This produces a characteristic '2:2:1' resonance pattern for the η^6-arene ligand, where a mirror plane, the lone symmetry element, reflects the two *ortho* and *meta* arene protons and is co-planar with the *para* proton. The large chemical shift dispersion for the η^6-arene ring protons, 1.3 ppm, is unusual in that the shielding range commonly exhibited by arene–ruthenium complexes is more often in the order of 0.3–0.6 ppm. For example the η^6-arene protons of the closely related $(\eta^6$-$C_6H_5CH_3)RuCl_2(PBu^n_3)$, show a multiplet between δ 5.6 and 4.96 ppm [26]. However, other complexes, which contain the η^6-toluene ligand, have displayed a similar ^{1}H-NMR signature to $[RuCl_2(PPh_2(CH_2)_3$-η^6-$C_6H_5)]$ where the η^6-$C_6H_5CH_3$ ring is subject to restricted rotation [22,25].

The substantial upfield shifts of the metal bound arene resonances relative to the free arene fragment arise from a combination of the following effects: the withdrawal of π-electron density from the aromatic ring by the metal resulting in a quenching of the ring currents by interaction with the metal, metal to arene π-interactions causing an increase in the total electron density at the aromatic ring and by the magnetic anisotropy of the rest of the complex. Although, it is considered that these explanations offer a rationale for the upfield shifts in such complexes, a more precise description is not yet available [27]. However, it is reasonable to expect that the magnitude of the shielding for the η^6-arene ligand will correlate closely with the electron density on the metal and the metal to arene π-interactions.

The ^{1}H-NMR spectrum for the η^6-arene group in **1** displayed a coupling pattern of three triplets and two doublets of relative intensities 1:1:1:1:1 (vicinal coupling, $^3J_{HH} = 6.4$–5.4 Hz), see Table 3. Complex **1** possess C_1 symmetry and as a result all five arene proton environments on the η^6-C_6H_5 group are unique. From the ^{1}H–^{1}H COSY spectrum it was possible to confirm that the triplet at δ 6.42 ppm was due to the *para* ring proton H_7, since it can be seen to be coupling strongly to the other two triplet signals at δ 6.11 and 6.02 ppm. The 2D-NMR experiment also showed the doublet at δ 5.84 ppm coupled to the triplet at δ 6.02 ppm and the doublet at δ 6.49 ppm coupled to the triplet at δ 6.11 ppm, giving the respective sets of *ortho* and *meta* protons on adjacent sides of the η^6-arene ring. In an effort to further assign these peaks it was necessary

Table 3
Selected ^{1}H-NMR data for complexes **1**–**6** (δ ppm)

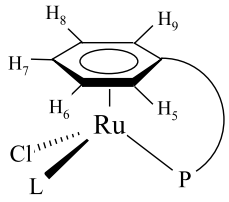

Complex	H_5	H_6	H_7	H_8	H_9
1	5.84 (d)	6.20 (t)	6.42 (t)	6.11 (t)	6.49 (d)
2	5.57 (d)	6.42 (m)	6.82 (t)	6.62 (t)	6.42 (m)
3	3.96 (d)	5.98 (t)	6.92 (t)	6.66 (t)	6.18 (d)
4	6.27 (d)	6.50 (m)	6.66 (t)	5.96 (t)	6.50 (m)
5	5.59 (d)	6.70 (t)	6.64 (t)	6.06 (t)	5.86 (d)
6	5.97 (d)	6.17 (t)	6.64 (t)	6.41 (t)	5.51 (d)

to consider the influence of the $P(OPh)_3$ ligand on the η^6-C_6H_5 ring. The *ortho* arene ring proton H_9 is *trans* to the $P(OPh)_3$ ligand on the ruthenium and since the phosphite will exert a *trans* influence due to its π-acid character [20], the electron density at this *ortho* position will be reduced. This will cause a decrease in the shielding effect of the ruthenium atom at this site. Consequently, one of the *ortho* protons is shielded relative to its counterpart on the opposite side of the arene ring and it is therefore proposed that the H_9 proton appears as the furthest downfield doublet at δ 6.49 ppm. The allocation of the remaining η^6-arene protons is then consistent with the assignments shown in Table 3.

The ^{1}H-NMR spectrum recorded for complex **2** showed four resonances which could be attributed to the η^6-arene group in a coupling pattern of two triplets, one multiplet and one doublet of relative intensities 1:1:2:1, respectively. The assignments given in Table 3 were verified using a ^{1}H–^{1}H COSY experiment and the multiplet centred at δ 6.42 ppm was identified as comprising of *meta* and *ortho* protons from opposite sides of the η^6-C_6H_5 ring and the triplet at δ 6.82 ppm was assigned to the *para* proton, H_7. The H_9 *ortho* proton, which lies *trans* to the $P(OMe)_3$ ligand, will experience deshielding and as a consequence appear as a downfield doublet. Hence, the multiplet at δ 6.42 ppm has been attributed to the overlap of the H_6 and H_9 protons.

The most noteworthy characteristic of the ^{1}H-NMR spectrum exhibited by **3** was the remarkably large chemical shift dispersion, 3 ppm, displayed by the η^6-arene ligand. Assignment of these resonances was again achieved from the ^{1}H–^{1}H COSY experiment, combined with a consideration of the influence of the PPh_3 ligand on the arene protons (see Table 3). ^{1}H-NMR studies of the analogous tethered cyclopentadienyl derivative $[RuCl(PPh_3)(PPh_2(CH_2)_2$-$\eta^5$-$C_5H_4)]$ [28], showed an unusual high-field resonance assignable to the η^5-C_5H_4 group at δ 2.29 ppm. The origin of this shift was ascribed to the anisotropic shielding effect of the aromatic ring current of a phenyl group in PPh_3. These effects are associated with the interaction of the cyclic delocalisation of the aromatic π-electrons of the phenyl groups in PPh_3 and nuclei, which lie directly above or below a phenyl ring and as a consequence are significantly shielded. A similar high-field shift was observed in the ^{1}H-NMR spectrum of **3**, showing a well-defined doublet at δ 3.96 ppm. The other spectra in this study do not contain such high-field arene signals, which can be assigned to the η^6-C_6H_5 ligand and it would appear that PPh_3 is responsible for this unusual chemical shift. By comparison with the cyclopentadienyl counterpart [28], it is plausible that this signal is due to an analogous shielding effect between one of the phenyl rings in PPh_3 and the *ortho* H_5 arene proton. Presumably, the tethered arene must orientate about the $[RuCl(PPh_3)(PPh_2(CH_2)_3)]$ tripodal set in solution to facilitate this type of intramolecular interaction. Related non-chelated complexes such as $[(\eta^6$-$C_6H_6)RuCl(PPh_3)(PMePh_2)][PF_6]$ [19c] fail to show analogous signals because of the rapid rotation about the Ru–arene bond; such rotation is of course not possible in these complexes. The spectrum for **3** also displayed an unexpected low-field resonance, showing a triplet at δ 6.92 ppm. The ^{1}H–^{1}H COSY spectrum was consistent with this signal arising from the H_7 proton in the *para* position of the co-ordinated arene ring. The 2D-NMR experiment also showed the doublet at δ 3.96 ppm coupled to the triplet at δ 5.98 ppm and the doublet at δ 6.18 ppm coupled to the triplet at δ 6.66 ppm, giving the respective sets of *ortho* and *meta* protons on adjacent sides of the η^6-arene ring. The appearance of the low-field triplets at δ 6.92 and 6.66 ppm, assigned to H_7 and H_6 respectively,

presumably results from the lifting free end of the η^6-C_6H_5 ring away from the ruthenium, as shown in the crystal structure of **3**.

The ^{1}H-NMR spectrum obtained for complex **4** displayed four resonances which could be attributed to the η^6-arene group in a coupling pattern of two triplets, one multiplet and one doublet of relative intensities 1:1:2:1, respectively. The assignments shown in Table 3 were consistent with ^{1}H–^{1}H correlation data, where the multiplet centred at δ 6.50 ppm was identified as comprising of an *meta* and *ortho* proton from opposite sides of the η^6-C_6H_5 ring and the triplet at δ 6.67 ppm was assigned to the *para* proton, H_7. The H_9 proton, which is *trans* to the PMe_3 ligand would be expected to experience deshielding due to the *trans* influence of the phosphine group, and appear as a downfield doublet. Therefore, the multiplet at δ 6.50 ppm can be ascribed to the overlap of the *meta* H_6 triplet and *ortho* H_9 doublet.

The *trans* influence exerted by the phosphine and phosphite ligands in complexes **1**–**4** can be attributed to their π-acceptor interactions via backdonation from a filled metal d-orbital on the Ru(II) centre to an empty orbital on the phosphorus ligand. This empty phosphorus orbital has been described as being an antibonding P–R σ orbital [29]. As electronegative groups are placed on the phosphorus atom, the energy of the P–R σ* orbital is lowered in energy, providing an increase in backbonding ability. The phosphorus ligands in **1**–**4** can be placed in the following order of π-acidity, $PMe_3 < PPh_3 < P(OMe)_3 < P(OPh)_3$, where triphenylphosphite has the greatest π-acceptor capability. Hence, it might be expected that complex **1** would show the most pronounced *trans* influence and exhibit the furthest downfield doublet in the ^{1}H-NMR spectra of **1**–**4**. Indeed the ^{1}H-NMR spectrum of **1** shows a downfield doublet at δ 6.49 ppm for the η^6-arene group, which has been assigned to the H_9 *ortho* proton. The ^{1}H-NMR spectra of complexes **2** and **4** both display downfield mutiplets at δ 6.42 and 6.50 ppm respectively, which have been attributed to the overlap of the H_9 and H_6 resonances. Whilst for **3** the H_9 proton appears as a doublet at δ 6.18 ppm. From this data it does not appear that there is any obvious correlation between the π-acidity of the phosphorus ligand and the deshielding of the H_9 *ortho* proton in the η^6-C_6H_5 ring. However, besides the electronic attributes of the phosphorus ligands, steric effects will also influence the degree of metal d to P–R σ* π overlap. Whereby the additional steric constraints of the larger ligands will hinder their approach towards the metal and limit the extent of π-backbonding. PPh_3 has the largest cone angle of the four phosphorus ligands used [30], which coincides with an upfield H_9 doublet in the ^{1}H-NMR spectrum of **3** (see Table 3). PPh_3 is not the weakest π-acid in this series, yet it appears to exert the poorest *trans* influence, due to the steric constraints around the ruthenium centre. Thus the magnitude of the *trans* deshielding influence displayed by these phosphorus ligands on the H_9 *ortho* proton exhibits interplay between both electronic and steric factors.

A distinctive feature of the ^{1}H-NMR spectrum recorded for **5** was the two adjacent triplets at δ 6.70 and 6.64 ppm (Table 3). The ^{1}H–^{1}H COSY spectrum was consistent with the signal at δ 6.64 ppm arising from the *para* H_7 proton. Further assignment of this spectrum required consideration of the magnetic anisotropic effects of the neighbouring groups in **5** and the shielding contributions attributed to the carbon–nitrogen triple bond in the MeCN ligand has two distinct susceptibilities, perpendicular and parallel to the bond axis [31]. If a hydrogen atom lies in a region parallel to the molecular axis it experiences deshielding and in a perpendicular orientation it is shielded. In **5** the *meta* H_6 proton of the η^6-arene ring occupies a position where it experiences deshielding from the carbon–nitrogen triple bond and it is proposed that this shifts the triplet due to this proton to low-field, producing the triplet at δ 6.70 ppm. The assignment of remaining peaks in this spectrum follows the labelling outlined in Table 3, verified by a ^{1}H–^{1}H COSY experiment. The H_9 proton, *trans* to the MeCN ligand appears at a high-field chemical shift, δ 5.86 ppm, compared to complexes **1**–**4**. This indicates that the *trans* influence exerted by MeCN was weak compared to the P-donor ligands, which matches the crystal structure data, where the Ru(1)–C(9) distance in **5** was shorter relative to **3** (see Tables 1 and 2).

The spectrum for the metal-bound arene group in **6** displayed five well-separated signals between δ 6.64 and 5.51 ppm and the allocation of these resonances is shown in Table 3. These assignments are consistent with the ^{1}H–^{1}H COSY spectrum and the anisotropic shielding effect attributed to the aromatic ring current in the pyridine ligand. The ^{1}H–^{1}H correlation data showed that the triplet at δ 6.17 ppm and the doublet at δ 5.97 ppm corresponded to a pair of adjacent *meta* and *ortho* protons on the same side of the η^6-arene ring. These two proton signals are displaying contrasting shielding effects compared to their counterparts on the opposite side of the η^6-C_6H_5 ligand. It is proposed that the aromatic ring current of the pyridine ligand would exert an intramolecular shielding affect upon the *meta* H_6 proton, where this nuclei lies in a region above the plane of the NC_5H_5 ring.

One additional aspect of the ^{1}H-NMR spectra for **1**–**6** that merits comment is the resonances assigned to the methylene protons in the chelating link. In most cases three independent multiplets were observed in the range δ 3.13–1.97 ppm, where the furthest downfield signals is allocated to the methylene group directly linked to the η^6-C_6H_5 ring, while the adjacent slightly further upfield

multiplet has been assigned the methylene groups attached to the phosphine. This assignment is consistent with related complexes, which contain a chelating η^1:η^6-phosphinoarene ligand [8,13,14]. The presence of diastereotopic methylene protons in these complexes is in agreement with C_1 symmetry at the ruthenium centre yielding a racemic chiral complex.

2.4. $^{13}C\{^1H\}$-NMR studies

For complexes **1**–**6** six resonances were observed for the η^6-C_6H_5 ligand in the $^{13}C\{^1H\}$-NMR spectra within the shielding range δ 106–79 ppm, confirming the C_1 molecular symmetry of these cations in solution. Table 4 highlights the assignments given to these ^{13}C resonances, which have been verified using ^1H–^{13}C correlation experiments. In the cases of **2** and **4**, a complete allocation of all the ^{13}C peaks was not possible, due to the overlap of some η^6-arene peaks in the ^1H-NMR spectra (Table 3). The *ipso* carbons, C_4, of the η^6-C_6H_5 ring for these complexes lied within the range δ 103–88 ppm. It is worth noting the ^{13}C spectra obtained for the η^6-C_6H_5 ring in **3**, see Table 4, where the three downfield resonances at δ 100.98, 99.39 and 99.29 ppm, have been assigned to the *para* C_7 carbon and the *meta* C_6 and C_8 carbons respectively. This data is consistent the long Ru–$C_{(arene)}$ distances shown in the structure of **3**, in particular for Ru–C6 and Ru–C7, where the free end of the arene is significantly lifted from the ruthenium. Three methylene resonances arising from the alkyl chelating link in the η^1:η^6-phosphinoarene ligand are observed in the range δ 30.7–19.02 ppm. The carbon bound directly to the phosphine can be easily identified as a well-defined doublet in the region δ 24.84–22.81 ppm ($^1J_{PC} = 34.7$–29.7 Hz).

3. Conclusions

In summary, the exchange of a chloride in $[RuCl_2(PPh_2(CH_2)_3$-η^6-$C_6H_5)]$, for the ligands L lowers the point symmetry at the ruthenium to C_1 and the ^1H- and ^{13}C-NMR spectra, in most cases, displayed a set of five and six signals assigned to the η^6-arene ring, respectively. The comparative chemical shifts of the ^1H- and ^{13}C-NMR resonances for complexes **1**–**6**, have demonstrated a high degree of sensitivity towards the chemical nature of the incoming ligands, L. Where ligands which are strong π-acids exhibit a significant *trans* influence on the η^6-C_6H_5 ring across the complex due to their ability to withdraw metal d_π-electrons. The magnetic anisotropic shielding attributed to the individual ligands also has an important effect on the chemical shifts of the co-ordinated arene nuclei.

4. Experimental

4.1. General

All syntheses were carried out under a dry nitrogen atmosphere using conventional Schlenk techniques. Reagents and solvents were obtained from normal commercial sources and were used without further purification unless otherwise stated. Diethyl ether was distilled from sodium, MeCN from CaH_2, and MeOH from magnesium turnings with iodine, all were stored under nitrogen. $[RuCl_2(PPh_2(CH_2)_3$-η^6-$C_6H_5)]$ was prepared by methods previously described in the literature [8]. Elemental analysis where performed by the Micro Analytical Laboratory, Department of Chemistry, The University of Manchester. All NMR spectra were recorded on a JEOL GSX Delta 270 MHz machine at ambient temperature and the $^{31}P\{^1H\}$-NMR spectra were referenced to H_3PO_4.

Table 4
Selected ^{1}C-NMR data for complexes **1**–**6** (δ ppm)

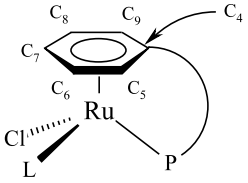

Complex	C_4	C_5	C_6	C_7	C_8	C_9
1	103.44	88.8	94.08	101.1	101.28	106.08
2	99.11	86.93	104.41/97.76	102.62	101.64	104.41/97.76
3	96.27	92.18	99.39	100.98	99.29	97.97
4	95.5	99.85	101.25/98.67	99.36	85.21	101.25/98.67
5	97.96	85.07	99.93	101.07	91.34	83.71
6	99.13	79.77	92.75	98.06	103.02	85.85

4.2. Synthesis of [RuCl(P(OPh)$_3$)(PPh$_2$(CH$_2$)$_3$-η^6-C$_6$H$_5$)][PF$_6$] (**1**)

A mixture of [RuCl$_2$(PPh$_2$(CH$_2$)$_3$-η^6-C$_6$H$_5$)] (100 mg, 0.21 mmol) and P(OPh)$_3$ (130 mg, 0.42 mmol) in the presence of NH_4PF_6 (68.4 mg, 0.42 mmol) in MeOH (20 ml) was refluxed for 1 h. The yellow solution was allowed to cool to room temperature (r.t.), filtered, concentrated under reduced pressure (5 ml) and Et_2O (50 ml) added giving a yellow microcrystalline solid, which was collected. This product was further purified by recrystallisation from a CH_2Cl_2–EtOH solvent mixture via slow evaporation and the yellow crystals were filtered from the mother liquor, washed with EtOH (2 × 5 ml) then dried under vacuum. Yield: 123 mg, 65%. Anal. Calc. for $C_{39}H_{36}ClF_6O_3P_3Ru$: C, 52.27; H, 4.05. Found: C, 52.92; H, 4.06%. ^{1}H-NMR (270 MHz, CD_3COCD_3, 298 K): δ 7.89–7.81 (m, 4H, Ph), 7.58–7.51 (m, 5H, Ph), 7.28–7.01 (m, 16H, Ph), 6.49 (d, $^3J_{HH} = 6.4$ Hz, 1H, *ortho* η^6-C$_6$H$_5$), 6.42 (t, $^3J_{HH} = 6.0$ Hz, 1H, *para* η^6-C$_6$H$_5$), 6.11 (t, $^3J_{HH} = 6.2$ Hz, 1H, *meta* η^6-C$_6$H$_5$), 6.02 (t, $^3J_{HH} = 6.0$ Hz, 1H, *meta* η^6-C$_6$H$_5$), 5.84 (d, $^3J_{HH} = 5.4$ Hz, 1H, *ortho* η^6-C$_6$H$_5$), 2.95 (m, 2H, Ph$_2$PCH$_2$CH$_2$C*H*$_2$-η^6-C$_6$H$_5$), 2.77 (m, 2H, Ph$_2$PC*H*$_2$CH$_2$CH$_2$-η^6-C$_6$H$_5$), 2.23 (m, 2H, Ph$_2$PCH$_2$C*H*$_2$CH$_2$-η^6-C$_6$H$_5$). ^{13}C{^{1}H}-NMR (68 MHz, CD_3COCD_3, 298 K): δ 152.03, 151.83, 135.37, 134.95, 134.81, 132.33, 130.47, 129.67, 129.59, 129.52, 128.66, 128.51, 126.48, 122.08, 122.02 (Ph), 106.08 (*ortho* η^6-C$_6$H$_5$), 103.04 (*ipso* η^6-C$_6$H$_5$), 101.28 (*meta* η^6-C$_6$H$_5$), 101.10 (*para* η^6-C$_6$H$_5$), 94.08 (*meta* η^6-C$_6$H$_5$), 88.80 (*ortho* η^6-C$_6$H$_5$), 29.51 (Ph$_2$PCH$_2$CH$_2$*C*H$_2$-η^6-C$_6$H$_5$), 24.62 (d, $^1J_{PC} = 33.7$ Hz, Ph$_2$P*C*H$_2$CH$_2$CH$_2$-η^6-C$_6$H$_5$), 19.67 (Ph$_2$PCH$_2$*C*H$_2$CH$_2$-η^6-C$_6$H$_5$). ^{31}P{^{1}H}-NMR (109 MHz, CD_3COCD_3, 298 K): δ 114.46 (d, $^2J_{PP} =$ 58.9 Hz, P(OPh)$_3$), 28.35 (d, $^2J_{PP} = 58.9$ Hz, Ph$_2$P(CH$_2$)$_3$-η^6-C$_6$H$_5$), −143.67 (sept, PF$_6$).

4.3. Synthesis of [RuCl(P(OMe)$_3$)(PPh$_2$(CH$_2$)$_3$-η^6-C$_6$H$_5$)][PF$_6$] (**2**)

This compound was prepared as for **1** from [RuCl$_2$(PPh$_2$(CH$_2$)$_3$-η^6-C$_6$H$_5$)] (100 mg, 0.21 mmol), P(OMe)$_3$ (52.1 mg, 0.42 mmol) and NH_4PF_6 (68.4 mg, 0.42 mmol) in MeOH (20 ml). Yield: 116 mg, 78%. Anal. Calc. for $C_{24}H_{30}ClF_6O_3P_3Ru$: C, 40.6; H, 4.26. Found: C, 40.49; H, 4.2%. ^{1}H-NMR (270 MHz, CD_3COCD_3, 298 K): δ 7.79–7.71 (m, 2H, Ph), 7.63–7.43 (m, 8H, Ph), 6.82 (t, $^3J_{HH} = 6.1$ Hz, 1H, *para* η^6-C$_6$H$_5$), 6.62 (t, $^3J_{HH} = 6.0$ Hz, 1H, *meta* η^6-C$_6$H$_5$), 6.42 (m, 2H, *ortho* and *meta* η^6-C$_6$H$_5$), 5.57 (d, $^3J_{HH} = 5.9$ Hz, 1H, *ortho* η^6-C$_6$H$_5$), 3.61 (d, $^3J_{PH} = 10.5$ Hz, 9H, P(OMe)$_3$), 2.87 (m, 2H, Ph$_2$PCH$_2$CH$_2$C*H*$_2$-η^6-C$_6$H$_5$), 2.46 (m, 2H, Ph$_2$PC*H*$_2$CH$_2$CH$_2$-η^6-C$_6$H$_5$), 2.05 (m, 2H, Ph$_2$PCH$_2$-C*H*$_2$CH$_2$-η^6-C$_6$H$_5$). ^{13}C{^{1}H}-NMR (68 MHz, CD_3COCD_3, 298 K): δ 134.06, 133.92, 133.06, 132.93, 130.39, 130.31, 127.74, 127.57 (Ph), 104.41 (*ortho* or *meta* η^6-C$_6$H$_5$), 102.62 (*para* η^6-C$_6$H$_5$), 101.64 (*meta* η^6-C$_6$H$_5$), 99.11 (*ipso* η^6-C$_6$H$_5$), 97.76 (*ortho* or *meta* η^6-C$_6$H$_5$), 86.93 (*ortho* η^6-C$_6$H$_5$), 54.31 (d, $^2J_{PC} = 8.8$ Hz, P(OMe)$_3$), 30.45 (Ph$_2$PCH$_2$CH$_2$*C*H$_2$-η^6-C$_6$H$_5$), 22.87, (d, $^1J_{PC} = 34.7$ Hz, Ph$_2$P*C*H$_2$CH$_2$CH$_2$-η^6-C$_6$H$_5$), 18.60 (Ph$_2$PCH$_2$*C*H$_2$CH$_2$-η^6-C$_6$H$_5$). ^{31}P{^{1}H}-NMR (109 MHz, CD_3COCD_3, 298 K): δ 121.58 (d, $^2J_{PP} =$ 86.3 Hz, P(OMe)$_3$), 27.36 (d, $^2J_{PP} = 86.4$ Hz, Ph$_2$P(CH$_2$)$_3$-η^6-C$_6$H$_5$), −143.81 (sept, PF$_6$).

4.4. Synthesis of [RuCl(PPh$_3$)(PPh$_2$(CH$_2$)$_3$-η^6-C$_6$H$_5$)][PF$_6$] (**3**)

This compound was prepared as for **1** from [RuCl$_2$(PPh$_2$(CH$_2$)$_3$-η^6-C$_6$H$_5$)] (100 mg, 0.21 mmol), P(Ph)$_3$ (110 mg, 0.42 mmol) and NH_4PF_6 (68.4 mg, 0.42 mmol) in MeOH (20 ml). Yield: 107 mg, 55%. Anal. Calc. for $C_{39}H_{36}ClF_6P_3Ru$: C, 55.23; H, 4.28. Found: C, 55.28; H, 4.32%. ^{1}H-NMR (270 MHz, CD_3COCD_3, 298 K): δ 7.93–6.97 (m, 25H, Ph), 6.92 (t, $^3J_{HH} = 6.2$ Hz, 1H, *para* η^6-C$_6$H$_5$), 6.66 (t, $^3J_{HH} = 6.4$ Hz, 1H, *meta* η^6-C$_6$H$_5$), 6.18 (d, $^3J_{HH} = 6.4$ Hz, 1H, *ortho* η^6-C$_6$H$_5$), 5.98 (t, $^3J_{HH} = 6.0$ Hz, 1H, *meta* η^6-C$_6$H$_5$), 3.96 (d, $^3J_{HH} =$ 5.7 Hz, 1H, *ortho* η^6-C$_6$H$_5$), 3.07 (m, 2H, Ph$_2$PCH$_2$-CH$_2$C*H*$_2$-η^6-C$_6$H$_5$), 2.34 (m, 4H, Ph$_2$PC*H*$_2$CH$_2$CH$_2$-η^6-C$_6$H$_5$, Ph$_2$PCH$_2$C*H*$_2$CH$_2$-η^6-C$_6$H$_5$). ^{13}C{^{1}H}-NMR (68 MHz, CD_3COCD_3, 298 K): δ 135.13, 135.03, 134.90, 134.71, 134.57, 134.44, 134.09, 133.97, 131.83, 131.52, 131.38, 129.52, 129.37, 129.18, 129.03 (Ph), 100.98 (*para* η^6-C$_6$H$_5$), 99.39 (*meta* η^6-C$_6$H$_5$), 99.29 (*meta* η^6-C$_6$H$_5$), 97.97 (*ortho* η^6-C$_6$H$_5$), 96.27 (*ipso* η^6-C$_6$H$_5$), 92.18 (*ortho* η^6-C$_6$H$_5$), 30.17 (Ph$_2$PCH$_2$CH$_2$*C*H$_2$-η^6-C$_6$H$_5$), 24.84 (d, $^1J_{PC} = 32.2$ Hz, Ph$_2$P*C*H$_2$CH$_2$CH$_2$-η^6-C$_6$H$_5$), 19.50 (Ph$_2$PCH$_2$*C*H$_2$CH$_2$-η^6-C$_6$H$_5$). ^{31}P{^{1}H}-NMR (109 MHz, CD_3COCD_3, 298 K): δ 22.92 (d, $^2J_{PP} =$ 51.1Hz, Ph$_2$P(CH$_2$)$_3$-η^6-C$_6$H$_5$), 17.49 (d, $^2J_{PP} = 51.3$ Hz, PPh$_3$), −143.59 (sept, PF$_6$).

4.5. Synthesis of [RuCl(PMe$_3$)(PPh$_2$(CH$_2$)$_3$-η^6-C$_6$H$_5$)][PF$_6$] (**4**)

This compound was prepared as for **1** from [RuCl$_2$(PPh$_2$(CH$_2$)$_3$-η^6-C$_6$H$_5$)] (100 mg, 0.21 mmol), PMe$_3$ (32 mg, 0.42 mmol) and NH_4PF_6 (68.4 mg, 0.42 mmol) in MeOH (20 ml). Yield: 86 mg, 62%. Anal. Calc. for $C_{24}H_{30}ClF_6P_3Ru$: C, 43.54; H, 4.57. Found: C, 43.25; H, 4.65%. ^{1}H-NMR (270 MHz, CD_3COCD_3, 298 K): δ 7.97–7.90 (m, 2H, Ph), 7.72–7.39 (m, 8H, Ph), 6.67 (t, $^3J_{HH} = 6.0$ Hz, 1H, *para* η^6-C$_6$H$_5$), 6.50 (m, 2H, *ortho* and *meta* η^6-C$_6$H$_5$), 6.27 (d, $^3J_{HH} = 5.7$ Hz, 1H, *ortho* η^6-C$_6$H$_5$), 5.69 (t, $^3J_{HH} = 6.0$ Hz, 1H, *meta* η^6-C$_6$H$_5$), 3.13 (m, 2H, Ph$_2$PCH$_2$CH$_2$C*H*$_2$-η^6-C$_6$H$_5$), 2.31 (m, 2H, Ph$_2$PC*H*$_2$CH$_2$CH$_2$-η^6-C$_6$H$_5$), 1.97 (m, 2H, Ph$_2$PCH$_2$C*H*$_2$CH$_2$-η^6-C$_6$H$_5$), 1.34 (d, $^2J_{PH} = 10.9$ Hz, 9H, PMe$_3$). ^{13}C{^{1}H}-NMR (68 MHz, CD_3COCD_3, 298

K): δ 135.11, 134.96, 134.04, 133.88, 131.95, 129.77, 129.62, 129.49, 129.34 (Ph), 101.25 (*ortho* or *meta* η^6-C_6H_5), 99.85 (*ortho* η^6-C_6H_5), 99.36 (*para* η^6-C_6H_5), 98.67 (*ortho* or *meta* η^6-C_6H_5), 95.5 (*ipso* η^6-C_6H_5), 85.21 (*meta* η^6-C_6H_5), 29.16 ($Ph_2PCH_2CH_2\mathit{C}H_2$-$\eta^6$-$C_6H_5$), 23.82 (d, $^1J_{PC} = 33.7$ Hz, $Ph_2P\mathit{C}H_2CH_2CH_2$-$\eta^6$-$C_6H_5$), 19.79 ($Ph_2PCH_2\mathit{C}H_2CH_2$-$\eta^6$-$C_6H_5$), 18.73 (d, $^1J_{PC} = 34.7$ Hz, PMe_3). $^{31}P\{^1H\}$-NMR (109 MHz, CD_3COCD_3, 298 K): δ 21.48 (d, $^2J_{PP} = 63.7$ Hz $Ph_2P(CH_2)_3$-η^6-C_6H_5, 3.46 (d, $^2J_{PP} = 62.1$ Hz, PMe_3), -143.92 (sept, PF_6).

4.6. Synthesis of [RuCl(NCMe)($PPh_2(CH_2)_3$-η^6-C_6H_5)][PF_6] (5)

This compound was prepared as for **1** from [$RuCl_2(PPh_2(CH_2)_3$-η^6-$C_6H_5)$] (100 mg, 0.21 mmol) and NH_4PF_6 (68.4 mg, 0.42 mmol) in MeCN (20 ml). Orange block-like crystals were obtained from a MeCN–Et_2O solvent mixture via slow vapour diffusion. Yield: 112 mg, 74%. Anal. Calc. for $C_{23}H_{24}ClF_6NP_2Ru$: C, 44.06; H, 3.86; N, 2.23. Found: C, 43.87; H, 3.87; N, 2.2%. IR (KBr): 2298 cm^{-1} [ν(NCMe)]. ^{1}H-NMR (270 MHz, CD_3COCD_3, 298 K): δ 7.78–7.49 (m, 10H, Ph), 6.70 (t, $^3J_{HH} = 6$ Hz, 1H, *meta* η^6-C_6H_5), 6.64 (t, $^3J_{HH} = 6.2$ Hz, 1H, *para* η^6-C_6H_5), 6.06 (t, $^3J_{HH} = 6.0$ Hz, 1H, *meta* η^6-C_6H_5), 5.86 (d, $^3J_{HH} = 5.8$ Hz, 1H, *ortho* η^6-C_6H_5), 5.59 (d, $^3J_{HH} = 5.8$ Hz, 1H, *ortho* η^6-C_6H_5), 3.06 (m, 2H, $Ph_2PCH_2CH_2C\mathit{H}_2$-$\eta^6$-$C_6H_5$), 2.66 (m, 2H, $Ph_2PC\mathit{H}_2CH_2CH_2$-$\eta^6$-$C_6H_5$), 2.47 (m, 2H, $Ph_2PCH_2C\mathit{H}_2CH_2$-$\eta^6$-$C_6H_5$); 2.25 (s, 3H, NCMe). $^{13}C\{^1H\}$-NMR (68 MHz, CD_3COCD_3, 298 K): δ 135.76, 133.66, 132.27, 131.58, 129.49, 128.93 (Ph), 126.95 (N*C*Me), 101.07 (*para* η^6-C_6H_5), 99.93 (*meta* η^6-C_6H_5), 97.96 (*ipso* η^6-C_6H_5), 91.34 (*meta* η^6-C_6H_5), 85.07 (*ortho* η^6-C_6H_5), 83.71 (*ortho* η^6-C_6H_5), 30.42 ($Ph_2PCH_2CH_2\mathit{C}H_2$-$\eta^6$-$C_6H_5$), 23.59 (d, $^1J_{PC} = 34.4$ Hz, $Ph_2P\mathit{C}H_2CH_2CH_2$-$\eta^6$-$C_6H_5$), 21.05 ($Ph_2PCH_2\mathit{C}H_2$-$CH_2$-$\eta^6$-$C_6H_5$); 3.32 (NC*Me*). $^{31}P\{^1H\}$-NMR (109 MHz, CD_3COCD_3, 298 K): δ 28.85 (s, $Ph_2P(CH_2)_3$-η^6-C_6H_5), -141.56 (sept, PF_6).

4.7. Synthesis of [RuCl(NC_5H_5)($PPh_2(CH_2)_3$-η^6-C_6H_5)][PF_6] (6)

This compound was prepared as for **1** from [$RuCl_2(PPh_2(CH_2)_3$-η^6-$C_6H_5)$] (100 mg, 0.21 mmol), Py (32.2 mg, 0.42 mmol) and NH_4PF_6 (68.4 mg, 0.42 mmol) in MeOH (20 ml). Yellow block-like crystals were obtained from a MeCN–Et_2O solvent mixture via slow vapour diffusion. Yield: 125 mg, 79%. Anal. Calc. for $C_{26}H_{26}ClF_6NP_2Ru$: C, 46.96; H, 3.94; N, 2.11. Found: C, 46.42; H, 3.69; N, 2.0%. ^{1}H-NMR (270 MHz, CD_3COCD_3, 298 K): δ 8.79 (dd, 2H, NC_5H_5), 7.77 (m, 1H, NC_5H_5), 7.69–7.11 (m, 10H, Ph), 7.08 (m, 2H, NC_5H_5), 6.64 (t, $^3J_{HH} = 6.1$ Hz, 1H, *para* η^6-C_6H_5), 6.41 (t, $^3J_{HH} = 6.2$ Hz, 1H, *meta* η^6-C_6H_5), 6.17 (t, $^3J_{HH} = 6.0$ Hz, 1H, *meta* η^6-C_6H_5), 5.97 (d, $^3J_{HH} = 5.9$ Hz, 1H, *ortho* η^6-C_6H_5), 5.51 (d, $^3J_{HH} = 5.8$ Hz, 1H, *ortho* η^6-C_6H_5), 2.95 (m, 2H, $Ph_2PCH_2CH_2C\mathit{H}_2$-$\eta^6$-$C_6H_5$), 2.64 (m, 2H, $Ph_2PC\mathit{H}_2CH_2CH_2$-$\eta^6$-$C_6H_5$), 2.03 (m, 2H, $Ph_2PCH_2C\mathit{H}_2CH_2$-$\eta^6$-$C_6H_5$). $^{13}C\{^1H\}$-NMR (68 MHz, CD_3COCD_3, 298 K): δ 156.78 (NC_5H_5), 139.23 (NC_5H_5), 135.78, 132.91, 131.98, 131.01, 129.36, 128.67 (Ph), 126.14 (NC_5H_5), 103.02 (*meta* η^6-C_6H_5), 99.13 (*ipso* η^6-C_6H_5), 98.06 (*para* η^6-C_6H_5), 92.75 (*meta* η^6-C_6H_5), 85.85 (*ortho* η^6-C_6H_5), 79.77 (*ortho* η^6-C_6H_5), 30.51 ($Ph_2PCH_2CH_2\mathit{C}H_2$-$\eta^6$-$C_6H_5$), 22.61 (d, $^1J_{PC} = 29.7$ Hz, $Ph_2P\mathit{C}H_2CH_2CH_2$-$\eta^6$-$C_6H_5$), 20.15 ($Ph_2PCH_2\mathit{C}H_2CH_2$-$\eta^6$-$C_6H_5$). $^{31}P\{^1H\}$-NMR (109 MHz, CD_3COCD_3, 298 K): δ 26.95 (s, $Ph_2P(CH_2)_3$-η^6-C_6H_5), -143.81 (sept, PF_6).

Table 5
Crystal and structure refinement data for complexes **3** and **5**

Complex	**3**	**5**
Empirical formula	$C_{39}H_{36}ClF_6P_3Ru$	$C_{23}H_{24}ClF_6NP_2Ru$
Formula weight	848.11	626.89
Temperature (K)	150(2)	150(2)
Wavelength (Å)	0.71073	0.71073
Crystal system	Monoclinic	Monoclinic
Space group	$P2_1/c$	$P2_1/c$
Unit cell dimensions		
a (Å)	9.45570(10)	7.78080(10)
b (Å)	20.0501(3)	21.7979(4)
c (Å)	18.4173(3)	14.2215(3)
α (°)	90	90
β (°)	91.9066(8)	90.4530(6)
γ (°)	90	90
V (Å^3)	3489.76(9)	2411.96(7)
Z	4	4
D_{calc} (mg m^{-3})	1.614	1.726
Absorption coefficient (mm^{-1})	0.725	0.953
F(000)	1720	1256
Crystal	Block, orange	Block, orange
Crystal size (mm^3)	$0.15 \times 0.12 \times 0.07$	$0.10 \times 0.07 \times 0.07$
θ Range for data collection (°)	2.96–26.00	3.01–26.00
Reflections collected	14 142	15 886
Independent reflections	6800 [$R_{int} = 0.0317$]	4730 [$R_{int} = 0.0410$]
Completeness to $\theta = 26.00°$	99.0%	99.3%
Max/min transmission	0.9510 and 0.8990	0.9363 and 0.9107
Refinement method	Full-matrix least-squares on F^2	Full-matrix least-squares on F^2
Data/restraints/parameters	6800/7/515	4703/0/332
Final R indices [$F^2 > 2\sigma(F^2)$]	$R_1 = 0.0418$, $wR_2 = 0.0896$	$R_1 = 0.0340$, $wR_2 = 0.0748$
R indices (all data)	$R_1 = 0.0491$, $wR_2 = 0.0927$	$R_1 = 0.0428$, $wR_2 = 0.0775$
Goodness-of-fit on F^2	1.019	1.024
Largest difference peak and hole (e Å^{-3})	1.637 and -1.589	1.230 and -0.674

4.8. X-ray crystallography

Details of crystal data collection and refinement are listed in Table 5. The intensity data for **3** and **5** were collected on a Nonius Kappa CCD area-detector diffractometer at the window of a rotating anode FR591 generator (Mo–K_α radiation, $\lambda = 0.71073$ Å at 150 K). The structures were solved by direct methods and refined on F^2 by full-matrix least-squares refinements [32,33].

5. Supplementary materials

Full details have been deposited with the Cambridge Crystallographic Data Centre, CCDC nos. 181837 and 181838 for the complexes **3** and **5**, respectively. Copies of this information may be obtained free of charge from The Director, CCDC, 12 Union Road, Cambridge CB2 1EZ, UK (Fax: +44-1223-336033; e-mail: deposit@ccdc.cam.ac.uk or www: http://www.ccdc.cam.ac.uk).

Acknowledgements

We thank Johnson Matthey Ltd. for the loan of $RuCl_3 \cdot 3H_2O$ and P.W. (Faculty of Science and Engineering Analytical Centre, Manchester Metropolitan University) for assistance with the NMR studies.

References

[1] (a) M.A. Bennett, Coord. Chem. Rev. 166 (1997) 225;
(b) M.A. Bennett, Compr. Organomet. Chem. II 7 (1995) 549;
(c) H. le Bozec, D. Touchard, P.H Dixneuf, Adv. Organomet. Chem. 29 (1989) 163.

[2] See for example: (a) J. Cossy, F. Eustache, P.I. Dalko, Tetrahedron Lett. 42 (2001) 5005;
(b) I. Moldes, E. de la Encarnación, J. Ros, Á. Alvarez-Larena, J.F. Piniella, J. Organomet. Chem. 566 (1998) 165;
(c) L. Plasseraud, G.J Süss-Fink, J. Organomet. Chem. 539 (1997) 163;
(d) G. Meister, G. Rheinwald, H. Stoeckli-Evans, G.J. Süss-Fink, J. Chem. Soc. Dalton Trans. (1994) 3215;
(e) M.A. Bennett, T-N. Huang, T.W. Turney, J. Chem. Soc. Chem. Commun. (1979) 312;
(f) M.A. Bennett, T-N. Huang, A.K. Smith, T.W. Turney, J. Chem. Soc. Chem. Commun. (1978) 582.

[3] See for example: (a) R. Noyori, M. Yamakawa, S. Hashiguchi, J. Org. Chem. 66 (2001) 7931;
(b) V. Ritleng, J.P. Sutter, M. Pfeffer, C. Sirlin, Chem. Commun. (2000) 129;
(c) L. Delaude, A. Demonceau, A.F. Noels, Marcomolecules 32 (1999) 2091;
(d) T. Naota, H. Taka, S.C. Murahashi, Chem. Rev. 98 (1998) 2599.

[4] E.T. Singewald, C.A. Mirkin, A.D. Levy, C.L. Stern, Angew. Chem. Int. Ed. Engl. 33 (1994) 2473.

[5] B. Cetinkya, S. Demir, I Ozdemir, L. Toupet, D. Semeril, C. Bruneau, P.H. Dixneuf, New J. Chem. 25 (2001) 519.

[6] C.M. Hartshorn, P.J. Steel, Angew. Chem. Int. Ed. Engl. 35 (1996) 2655.

[7] Y. Miyaki, T. Onishi, H. Kurosawa, Inorg. Chim. Acta 300–302 (2000) 369.

[8] P.D. Smith, A.H. Wright, J. Organomet. Chem. 559 (1998) 141.

[9] B. Therrien, T.R. Ward, M. Pilkington, C. Hoffmann, F. Gilardoni, J. Weber, Organometallics 17 (1998) 330.

[10] (a) D. Jan, L. Delaude, F. Simal, A. Demonceau, A.F. Noels, J. Organomet. Chem. 606 (2000) 55;
(b) F. Simal, D. Jan, A. Demonceau, A.F. Noels, Tetrahedron Lett. 40 (1999) 1653.

[11] A. Fürstner, M. Liebl, C.W. Lehmann, M. Picquet, R. Kunz, C. Bruneau, D. Touchard, P.H. Dixneuf, Chem. Eur. J. 6 (2000) 1847.

[12] A. Abele, R. Wursche, M. Klinga, B. Rieger, J. Mol. Catal. Sect. A 160 (2000) 23.

[13] K.Y. Ghebreyessus, J.H. Nelson, Organometallics 19 (2000) 3387.

[14] M.A. Bennett, A.J. Edwards, J.R. Harper, T. Khimyak, A.C. Willis, J. Organomet. Chem. 629 (2001) 7.

[15] R.M. Bellabarba, G.C Saunders, S. Scott, Inorg. Chem. Commun. 5 (2002) 15.

[16] (a) M.A. Bennett, L.Y. Goh, A.C. Willis, J. Am. Chem. Soc. 118 (1996) 4984;
(b) M.A. Bennett, L.Y. Goh, A.C. Willis, J. Chem. Soc. Chem. Commun. (1992) 1180.

[17] J.H. Nelson, K.Y. Ghebreyessus, V.C. Cook, A.J. Edwards, W. Wielandt, S.B. Wild, A.C. Willis, Organometallics 21 (2002) 1727.

[18] (a) B. Therrien, T.R. Ward, Angew. Chem. Int. Ed. Engl. 38 (1999) 405;
(b) B. Therrien, A. König, T.R. Ward, Organometallics 18 (1999) 1565.

[19] (a) H. Werner, R. Werner, Chem. Ber. 115 (1982) 3766;
(b) H. Werner, R. Werner, J. Organomet. Chem. 174 (1979) C67;
(c) H. Werner, R. Werner, Angew. Chem. Int. Ed. Engl. 17 (1978) 683.

[20] M.A. Bennett, G.B Robertson, A.K. Smith, J. Organomet. Chem. 43 (1972) C41.

[21] J.C. McConway, A.C. Skapski, L. Philips, R.J. Young, G. Wilkinson, J. Chem. Soc. Chem. Commun. (1974) 327.

[22] A.R. Siedle, R.A. Newark, L.H. Pignolet, D.X. Wang, T.A. Albright, Organometallics 5 (1986) 38.

[23] R.V. Emanuel, E.W. Randall, J. Chem. Soc. Sect. A (1969) 3002.

[24] A. Wu, E.R. Biehl, P.C. Reeves, J. Organomet. Chem. 33 (1971) 53.

[25] See for example: (a) J.R. Polam, L.C. Porter, Inorg. Chim. Acta 205 (1993) 119;
(b) I.S. Thorburn, S.J. Rettig, B.R. James, J. Organomet. Chem. 296 (1985) 103.

[26] M.A. Bennett, A.K. Smith, J. Chem. Soc. Dalton Trans. (1974) 233.

[27] M.M. Maricq, J.S. Waugh, J.L. Fletcher, M.J. McGlinchey, J. Am. Chem. Soc. 100 (1978) 6902.

[28] A.M.Z. Slawin, D.J. Williams, J. Crosby, J.A. Ramsden, C. White, J. Chem. Soc. Dalton Trans. (1988) 2491.

[29] A.G. Orpen, N.G. Connelly, J. Chem. Soc. Chem. Commun. (1985) 1310.

[30] C.A. Tolman, Chem. Rev. 77 (1977) 313.

[31] W. Kemp, NMR in Chemistry, Macmillan Education, London, 1986.

[32] P.T. Beurskens, G. Beurskens, W.P. Bosman, R. de Gelder, S. Garcia-Granda, R.O. Gould, R. Israël, J.M.M. Smits, DIRDIF-96, Crystallography Laboratory, University of Nijmegen, The Netherlands, 1996.

[33] G.M. Sheldrick, SHELXL-97, University of Göttingen, Germany, 1997.